

# Design of Fourth Order Active Band-Pass Filter With Sallen and Key Topology

Y. A. Durrani<sup>1</sup>

<sup>1</sup>Electronics Engineering Department, UET, Taxila, Pakistan  
<sup>1</sup>yaseer.durrani@uettaxila.edu.pk

**Abstract**-Analog active filters can be found in most of the electronic circuits. One major application of active filters involve an important class of sharp cutoff filter used to condition analog input signals that are being sampled and converted to digital signal as real-time to the modern computers. In this paper, we present the design of active filter with the second and the fourth order Butterworth responses in the category of Sallen and Key filter architecture. This type of filter has voltage controlled voltage source topology that uses a unity-gain amplifier. The complex transfer function of the filter is obtained and the capacitor/ resistor values are calculated. The filter is simulated with the Multisim program and compared with the Matlab tool. The results of the frequency responses are very similar to each other.

**Keywords**-Active Filters, Sallen and Key Topology, Butterworth Response, Frequency Response, Power Estimation

## I. INTRODUCTION

Analog active filters can be found in most of the electronic circuits. In communication system, filters are generally used for the elimination of noise and tuning in specific frequencies of range (0 KHz to 20 KHz). In digital signal processing system, filters are implemented for interference and noise prevention. All input signals are composed of sinusoidal components of various frequencies, amplitudes and phases. If we are interested in a certain range of frequencies, we can design filters to eliminate frequency elements outside the range. Active filters can be made to be part of adaptive signal-processing systems. Here the filter's poles, zeros or gain can be altered electronically in response to some criterion. A tracking active filter can be made to follow the frequency of a coherent input to preserve maximum signal-to-noise ratio at the filter's output. One major application of active filters involves an important class of sharp cutoff low-pass filter used to condition analog input signals that are being periodically sampled and converted to digital form as real-time inputs to digital computers. Anti-aliasing filters remove all significant signal spectral energy at and above one-half the sampling frequency. Active filters can also be made to be part of adaptive signal-

processing systems. A tracking active filter can be made to follow the frequency of a coherent input signal to preserve maximum signal-to-noise ratio at the filter's output.

Numerous types of filter designs have evolved in the past twenty years. Most of them are non-standard and less precise values of resistors and capacitors to achieve design goals. Among those active filters are most effective filters. Active filter uses operational amplifier (op-amp) as active component in the circuit. Op-amp-based active filters do not require the use of inductances in their designs. It is far easier to build a nearly ideal resistor or capacitor than an ideal inductor. Also, inductors are bulky and heavy. Thus modern active filter use only resistors, capacitors and op-amps that can make compact and inexpensive relative to RLC networks with the same pole-zero platforms. This is especially true when we consider filters designed to work in the subsonic spectral region. Also, design procedures for high-order, passive RLC filter are very complex, whereas the modular approach used in the synthesis of high-order active filters makes design more straightforward.

Some types of filters have no independent control of mid-band gain, damping factor, or break frequency. The most popular types of active filter responses are the Tschebyscheff, Chebyshev, Bessel and Butterworth. Among these, Butterworth is most effective topology for the implementation of the maximum flat response. It exhibits a nearly no ripples with flat pass. The roll-off is more monotonic and smooth with high-pass and low-pass roll of 20 dB/decade for each pole. Thus, the implementation of filter with fourth order would have attenuation rate of +40 dB/decade and -40 dB/decade. The filter responses can be demonstrated with band-pass, band-stop, low-pass, and high-pass filter configuration setups.

The paper is organized as follows. In Section II and III, the background of Butterworth filter and Sallen and Key filter is discussed. In Section IV and V, the analysis of the active low-pass and band-pass filters are described. The implementation of the fourth order active band-pass filter using Sallen and Key topology is given in section VI. The power estimation method for filter and the results are discussed in Section VII and VIII. Finally, the Section IX summarizes the work.

## II. BUTTERWORTH FILTERS

Fig. 1 plots the amplitude and phase responses of Butterworth low-pass first order, and fourth order active filters [1, v]. The Butterworth filter has the maximum pass-band flatness as illustrated in the figure. Due to the flatness, it uses as anti aliasing filter in data conversion applications with preciseness in the signal across the entire pass-band. Many low-pass filters are designed to construct with a Butterworth transfer function with following magnitude response:

$$|H(f)| = \frac{H_o}{\sqrt{1+f/f_b^{2n}}} \quad (1)$$

where  $n$  is the order of the filter and  $f_b$  the 3 dB cutoff frequency and  $H_o$  is the gain magnitude at dc voltage.

Active low-pass Butterworth filter response can be implemented by cascading modified Sallen and Key circuits. In this class of active filter, an op-amp is used to provide voltage-controlled voltage-source (VCVS) with a low inverting or non-inverting voltage gain, and along with various resistors and capacitors, to realize quadratic low-pass, band-pass and high-pass filters. This class includes the well-known Sallen and Key designs, which are described in the next sections.

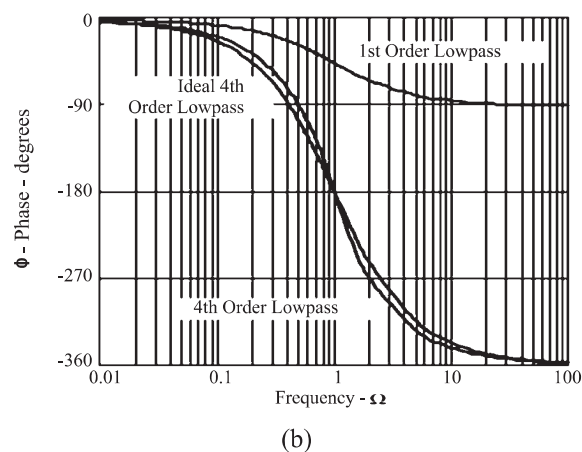
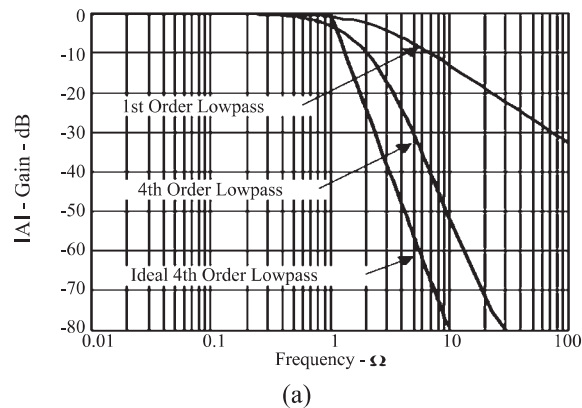


Fig. 1. Frequency responses of 1<sup>st</sup> and 4<sup>th</sup> order active low pass filters with (a) magnitudes and (b) phases [1]

## III. SALLEN AND KEY VCVS FILTERS

The second-order Sallen and Key electronic filters are the degenerated form of a VCVS filter topology. A VCVS filters generally uses a unity gain voltage amplifier with the high input impedance, zero output impedance, and the infinite impedance of input to implement a two-pole (12 dB/octave) low-pass, band-pass or high-pass responses. This unity-gain amplifier (i.e., a pure buffer amplifier with 0 dB gain) permits for high Q-factor and pass-band gain without the use of inductors in the analog circuits. However, source or emitter followers are different choices for the buffer amplifier. Voltage-controlled voltage-source filters are comparatively resilient to certain level of the component tolerance. Due to the consideration of high Q-factor may need extreme individual component value or high gain [ii, v]. Higher order filters can be constructed by cascading two or more stages as shown in figure 7. The filter cascaded order may be increases up to 10<sup>th</sup> order by cascading first and second order type. However, identical stages are not recommended and rarely can be used due to very poor frequency response for different applications.

### A. Characterizations of Sallen and Key filter

- Positive gain or non-inverting amplifier
- Components replication
- Simplicity in analog designs

### B. Limitations of the filter

- The gain and Q-factor are related to each other
- Q-factor > 0.5, since  $A_v > 1$

## IV. LOW-PASS FILTERS

A Sallen and Key quadratic low-pass filter with non-inverting VCVS can easily be made with an op-amp and two resistors/capacitors (RC) as illustrated in Fig. 2. The frequency response of the ideal low-pass filter is shown in Fig. 3. Analysis of the behavior of active filter design proceeds by noting:

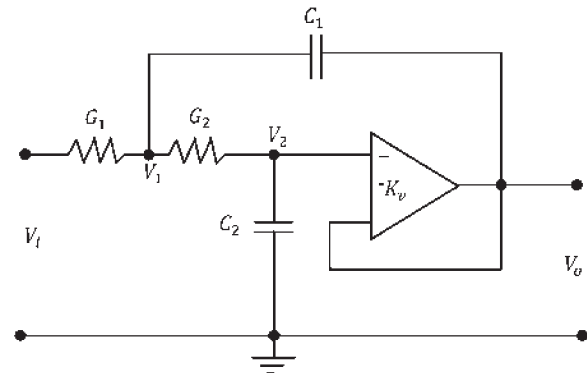


Fig. 2. Unity gain Sallen and Key VCVS low-pass active filter

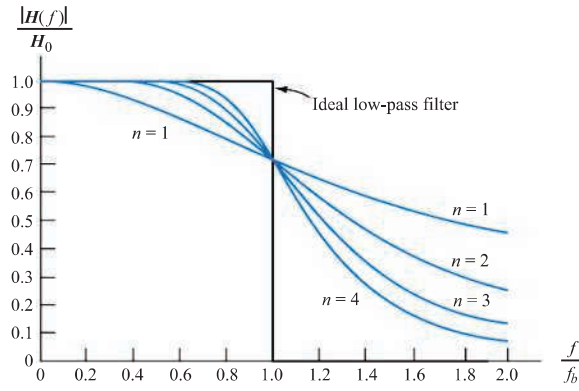


Fig. 3. The frequency response of low-pass Sallen and Key VCVS filter [iii]

Consider the low-pass filter design in Fig. 2, that  $V_O = K_v V_2$  and

$$V_2 = \frac{V_1(1/sC_2)}{R_2 + 1/sC_2} = \frac{V_1}{1 + sR_2C_2} \quad (2)$$

Using Kirchoff's current law in (3):

$$V_1 \left( G_1 + \frac{1}{R_2 + 1/sC_2} + sC_1 \right) - sC_1 V_O = V_i G_1 \quad (3)$$

To solve (2) for  $V_1$  and substitute into (3), we find (4):

$$(sR_2C_2 + 1) \left( \frac{V_O}{K_v} \right) \left( G_1 + \frac{sC_2}{1 + sR_2C_2} + sC_1 \right) - sC_1 V_O = V_i G_1 \quad (4)$$

Then we can write the low-pass active filter's transfer function in time-constant format in (5):

$$\frac{V_O}{V_i} = \frac{K_v}{s^2 C_1 C_2 R_1 R_2 + s[C_2(R_1 + R_2) + R_1 C_1(1 - K_v)] + 1} \quad (5)$$

To solve it in Sallen and Key format,  $K_v = 1$ , so the filter's transfer function reduce to

$$\frac{V_O}{V_i} = \frac{1}{s^2 C_1 C_2 R_1 R_2 + s[C_2(R_1 + R_2)] + 1} \quad (6)$$

This filter's break frequency can be written in (7):

$$\omega_n = \sqrt{\frac{1}{C_1 C_2 R_1 R_2}} \quad (7)$$

and the damping frequency can be expressed in (8):

$$\xi = \frac{C_2(R_1 + R_2)}{2} \sqrt{\frac{1}{C_1 C_2 R_1 R_2}} \quad (8)$$

If  $R_1 = R_2$ , so that  $R_1 = R_2 = R$  then damping frequency reduces in (9):

$$\xi = \sqrt{\frac{C_2}{C_1}} \quad (9)$$

Hence the ratio  $C_2/C_1$  sets the Sallen and Key low-pass filter' damping factor, and simultaneous adjustment of  $R_1$  and  $R_2$  with a ganged, dual-variable resistor can set  $\omega_n$  independently of  $\xi$ . The dc gain of this low-pass filter is unity. During design, the value of the capacitance can be chosen first after resistance

values. As  $K_v$  increases from 0 to 3, the transfer function shows more peak values. In case of  $K_v > 3$ , then the circuit is not stable. The empirical values for filter can be determined with the combination of different orders.

#### A. The Butterworth Approximation

The general form of the non-zero transfer function of nth-order low-pass filter is shown in (10) [iv]:

$$A(s) = K \frac{1}{1 + \mu_1(s/\omega_c) + \mu_2(s/\omega_c)^2 + \dots + \mu_n(s/\omega_c)^n} \quad (10)$$

where  $K$  is the dc gain constant,  $\omega_c$  is a normalization frequency, and the  $\mu_i$  are the positive constants.

#### B. High-Pass Filter

Fig. 4 illustrates a Sallen and Key high-pass filter. Following a nodal analysis similar to just used on the low-pass filter, we obtain the following transfer function, where we assume  $K_v$  and  $C_1 = C_2 = C$  in (11):

$$\frac{V_O}{V_i} = \frac{s^2 C_1 C_2 R_1 R_2}{s^2 C_1 C_2 R_1 R_2 + s(C_1 R_1 + C_2 R_1) + 1} \quad (11)$$

Here again, the undamped natural frequency of the filter is expressed in (12):

$$\omega_n = \sqrt{\frac{1}{C_1 C_2 R_1 R_2}} \quad (12)$$

and the damping frequency is in (13):

$$\xi = \frac{R_1(2C)}{2} \sqrt{\frac{1}{C R_1 R_2}} = \sqrt{\frac{R_1}{R_2}} \quad (13)$$

The high-frequency ( $\omega \gg \omega_n$ ) gain for this filter is also unity.

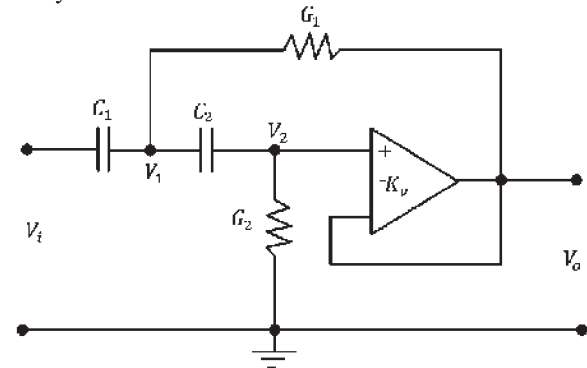


Fig. 4. Unity gain Sallen and Key VCVS high-pass active filter

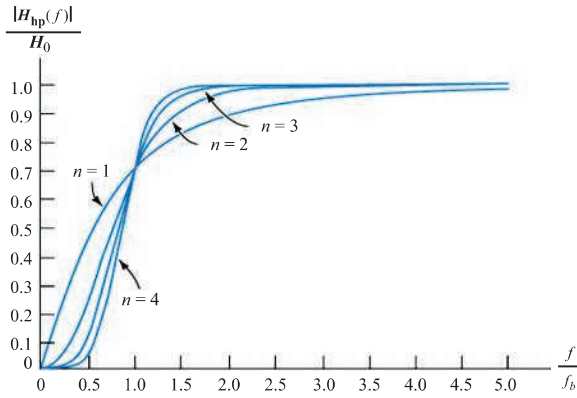


Fig. 5. The frequency response of low-pass Sallen and Key VCVS filter [3].

### V. BAND-PASS ACTIVE FILTER

The unity gain Sallen and Key VCVS band-pass active filter is shown in Fig. 6.

By solving the circuit of Fig. 6, the node equation for  $V_1$  and  $V_2$ , noting that  $V_o = K_v V_2$ , we find in (14):

$$\frac{V_o}{V_i} = \frac{s \left[ \frac{K_v C_1 G_1}{G_2(G_1 + G_3)} \right]}{s^2 \left[ \frac{C_1 C_2}{G_2(G_1 + G_3)} \right] + s \left[ \frac{C_1 G_2 + (C_1 + C_2)(G_1 + G_3) - K_v C_1 G_3}{G_2(G_1 + G_3)} \right] + 1} \quad (14)$$

where we assume  $K_v = 2$  and  $C_1 = C_2 = C$  in (15):

$$\omega_n = \frac{1}{C} \sqrt{G_2(G_1 + G_3)} \quad (15)$$

$$A_v = \frac{2G_1}{G_2 + 2G_1} \quad (16)$$

and the damping frequency is (17):

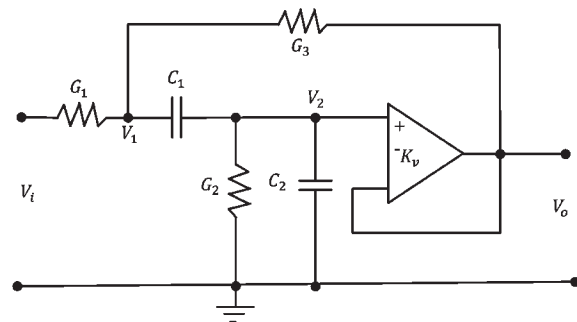


Fig. 6. Unity gain Sallen and Key VCVS band-pass

$$Q = \frac{G_2(G_1 + G_3)}{\sqrt{G_2(G_1 + G_3)(G_2 + 2G_1)}} \quad (17)$$

Note that the peak response  $A_v$  and  $Q$  are independent of  $C$ ;  $C_1 = C_2 = C$  can be used to set  $\omega_n$  at  $A_v$  and  $Q$ .

### VI. IMPLEMENTATION OF 4TH ORDER ACTIVE BAND-PASS FILTER CIRCUIT USING SALLEN-KEY TOPOLOGY

The filter cascaded order may be increases up to

10<sup>th</sup> order by cascading first and second order type. However, identical stages are not recommended and rarely can be used due to very poor frequency response for different applications. The design of 4<sup>th</sup> order filter is very complex, it may be designed by the cascading two second-order filters as shown in figure 7. The attenuation at the cutoff frequency of individual filter should be -3dB then the attenuation for two stage filter will be at -6dB.

TABLE I  
SPECIFICATIONS OF BAND-PASS FILTER

Specifications	Values
Pass-band frequency	10-20 KHz
Pass-band ripples	0.5 dB
Stop-band attenuation	60 dB
Center frequency	17 kHz
Overall Mid frequency	15 kHz

The design of 4<sup>th</sup> order active band-pass filter of Sallen and Key topology is implemented in this paper due to its simplicity of the design. The Butterworth filter response is adopted for more flat gain. These types of filter response have wider range during the lower order with low-power dissipation and good linearity. The filter response is insensitive to parasitic capacitances. The second order Sallen and Key band-pass filter is illustrated in Fig. 6. The specifications of desired filter are shown in Table I.

The transfer function of 4<sup>th</sup> order active band-pass filter is determined in (18):

$$A_v = \frac{\frac{A_{mid} \sigma_s}{Q_p}}{\left[ \frac{1}{Q_p} \left( \frac{s}{\sigma} \right) + \left( \frac{s}{\sigma} \right)^2 + 1 \right]} \cdot \frac{\frac{A_{mid} \sigma_s}{Q_p}}{\left[ \frac{\sigma s}{Q_p} + (\sigma s)^2 + 1 \right]} \quad (18)$$

where  $A_{mid}$  is the gain of mid frequency  $f_{mid}$  of individual filter,  $Q_p$  is the quality of pole for each filter,  $\sigma$  and  $1/\sigma$  are the mid frequency factors of individual filters  $f_{mid-1}$  and  $f_{mid-2}$  extracted from the  $f_{mid}$  of the overall band-pass filter.

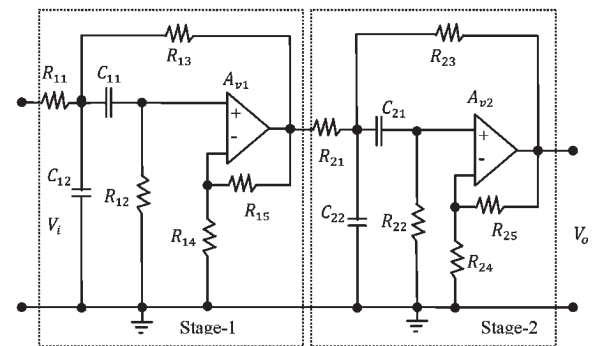


Fig. 7. Sallen and Key VCVS 4<sup>th</sup> order band-pass active filter



Using successive approximation method, factor  $\sigma$  is derived in (19):

$$\sigma^2 + \frac{1}{\sigma^2} + \left[ \frac{\sigma \alpha_1 \Delta\varphi}{\beta_1(1+\sigma^2)} \right]^2 - \frac{(\Delta\varphi)^2}{\beta_1} - 2 = 0 \quad (19)$$

where  $\Delta\varphi$  is the normalized bandwidth defined as  $\Delta\varphi = (Q_{all})^{-1}$ , ( $Q_{all} = 1.5$ ) is the overall filter's quality),  $\alpha_1$  and  $\beta_1$  are the second order low-pass coefficients of the specific desired filter type. In this case Butter worth filter has  $\alpha_1 = 1.4142$  and  $\beta_1 = 1$ . The overall filter's quality in (20):

$$Q_{all} = \frac{f_{mid}}{B} \quad (20)$$

The quality of each filter can presented in (21):

$$Q_p = Q_{all} \cdot \frac{\beta_1(1+\sigma^2)}{\sigma \alpha_1} \quad (21)$$

The individual gain of the mid frequencies  $f_{mid-1} = f_{mid-2} = f_{mid}$  is same for both filters, so

$$A_{mid} = \frac{Q_p}{Q_{all}} \cdot \left( \sqrt{\frac{A_m}{\beta_1}} \right) \quad (22)$$

where  $A_m$  is the overall gain at mid frequency taken as 2 value.

By using Table I,  $\sigma = 1.27$ ,  $Q_p = 2.28$ ,  $A_{mid} = 4.12$ . In Fig. 7, the RC values are calculated for both stages of 4<sup>th</sup> order band-pass active filter as:

$$C_{11} = C_{12} = C_{21} = C_{22} = 10 \text{ nF}$$

$$R_{11} = R_{13} = 1.45 \text{ k}\Omega, R_{12} = 3.12 \text{ k}\Omega, R_{14} = 10 \text{ k}\Omega, R_{15} = 12.38 \text{ k}\Omega$$

$$R_{21} = R_{23} = 755.10 \text{ k}\Omega, R_{22} = 1.90 \text{ k}\Omega, R_{24} = 10 \text{ k}\Omega, R_{25} = 12.38 \text{ k}\Omega$$

The transfer function of 4<sup>th</sup> order Butterworth band-pass filter was derived as:

$$A_v = \frac{s^2 - 1}{s^2 - 0.6325s + 0.6597} \cdot \frac{s^2 - 1}{s^2 - 0.1155s + 0.6314} \quad (23)$$

Hence, by the use of transfer function in (23), the frequency response of the filter is plotted in Matlab tool as shown in Figure.

## VII. POWER ESTIMATION FOR FILTER

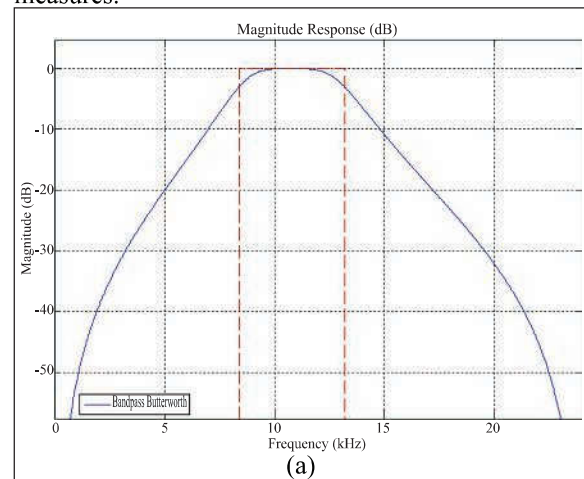
In this section, we present the power estimation procedure for Sallen and Key filter. Recently we have presented a macro-model for different intellectual property (IP) blocks and IP-based digital systems in [vi, vii, viii]. We used the same approach for the power estimation of the DSP applications such as Sallen and Key filter. In this method the statistical variables such as signal probability ( $SP$ ), transition density ( $TD$ ), spatio-temporal correlation ( $ST\_C$ ), are used for the

generation of input signals of the filter. Using functional simulations and power estimator, the output signal sequences are observed and the average power dissipation of the filter is estimated. The results of the filter are given in section VIII.

## VIII. EXPERIMENTAL RESULTS

This section demonstrates the results of 4<sup>th</sup> order band-pass Sallen and Key architecture with Butterworth response. The Butterworth filter response is adopted due to its flatter gain. The filter response has wider range during the lower order with low-power dissipation, good linearity and insensitive to the parasitic capacitances. The circuit of the band-pass filter is shown in figure 7. The filter consists of two stages of cascaded band-pass filters. It is designed with careful considerations for the adjustable values of the resistors/capacitors and constructed its transfer function in (23). The specification of the filter is shown in Table I. The result of the transfer function is illustrated in terms of the different plots of: magnitude, phase, step response and delay response as shown in figure 8. The filter is simulated in Multisim software and the transfer function is implemented in Matlab tool. The filter has band-pass frequencies 10KHz and 20 KHz, The band-pass gain is kept greater than one and roll-off rates of  $\pm 40$  dB/dec. The experimental result shows that the responses of the complex filter are very similar with the commercial software plots and shows accurate results in terms of flat gain.

We have implemented the statistical power estimation method of the filter as discussed in section VII. We have generated several randomly input signals of ( $SP$ ), ( $TD$ ), and ( $ST\_C$ ) of range between [0-1]. In experiments the average error of filter is found 11.34%. One important source of error is due to the power consumption of interconnects and the fixed coefficients used in the filter. The experiment demonstrates that the transition density is more significant in the estimation of power dissipation and relatively linear to the power measures.



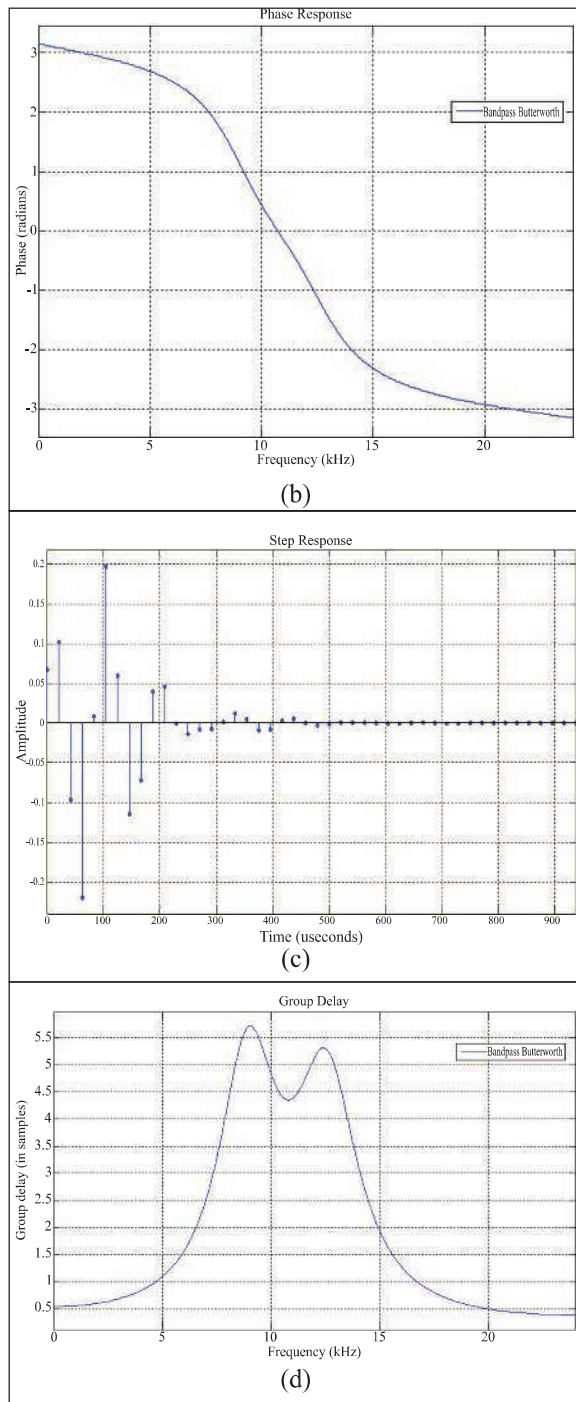


Fig. 8. Frequency responses of 4<sup>th</sup> order active band-pass filters with (a) magnitudes (b) phases (c) step response and (d) delay responses.

### IX. CONCLUSION

The 4<sup>th</sup> order band-pass filter is designed and simulated in this paper. The circuit of the filter is composed of two operational amplifiers, ten resistors, and four capacitors. The magnitude and phase

responses of the filter are very similar to the Multisim software. If more-accurate frequency response is required, more stages must be used. Power estimation of the filter is dependent on the digital input signals and greatly influence on the average power. The power estimation of the DSP applications is not only the transition activity at the inputs and outputs, but also the input arrival times and the spatio-temporal correlation of the input data.

### REFERENCES

- [i] T. Kugelstadt, “Active filter design techniques” *Report of Texas instruments, Literature number SLOA088*, Chapter 16, pp. 4-5, 2004.
- [ii] P. Löwenborg, O. Gustation, and L. Wanhammar “Filter Design Using MATLAB” *Radiovetenskap och Kommunikation 99, Karlskrona*, pp. 34-47, 1999.
- [iii] G. F. Miner and D. J. Comer, “Physical Data Acquisition for Digital Processing” *Prentice Hall Publisher*, Englewood Cliffs, NJ, 1992.
- [iv] R. Weinstein, “RFID: A technical overview and its applications to enterprise” *IEEE Computer Society*, Vol. 7, issue 3, pp. 27-33, 2005.
- [v] Y. A. Durrani, and T. Riesgo, “Power estimation technique for DSP architecture” *Elsevier Journal of digital signal processing*, Vol. 19, Issue 2, pp.213-219, 2009.
- [vi] Y. A. Durrani, and T. Riesgo “High-level power Analysis for IP-based digital systems” *Journal of Low Power Electronics, American Scientific Publisher*, Vol. 9, no. 4, pp. 435-444, 2013.
- [vii] Y. A. Durrani, and T. Riesgo “Power estimation for intellectual property-based digital systems at architectural level” *Elsevier Journal of King Saud University-Computer and Information Sciences*, Vol. 26, No. 3, pp. 287-295, 2014.
- [viii] Y. A. Durrani, and T. Riesgo, “High-level power analysis for intellectual property-based digital systems” *Springer Circuits, Systems & Signal Processing*, Vol. 32, no. 6, 2014.